Energy 215 (2021) 119095

Contents lists available at ScienceDirect

Energy

journal homepage: www.elsevier.com/locate/energy

Optimal planning of thermal energy systems in a microgrid with seasonal storage and piecewise affine cost functions

Muhammad Mansoor [a, b, *], Michael Stadler [a, c, d], Michael Zellinger [a], Klaus Lichtenegger [a, e], Hans Auer [b], Armin Cosic [a]

[a] BEST-Bioenergy and Sustainable Technologies GmbH, Gewerbepark Haag 3, 3250, Wieselburg-Land, Austria
[b] Energy Economics Group, Institute of Energy Systems and Electrical Drives, Vienna University of Technology, Gußhausstraße 25 – 29/E37003, 1040, Vienna, Austria
[c] Xendee Corporation, 6540 Lusk Blvd., Suite C225, San Diego, CA, 92121, USA
[d] Center for Energy and Innovative Technologies (CET), Austria
[e] FH Joanneum – University of Applied Sciences, Institut für Informationsmanagement, Eckertstraße 30i, 8020, Graz, Austria

ARTICLE INFO

Article history:
Received 20 May 2020
Received in revised form
5 October 2020
Accepted 14 October 2020
Available online 19 October 2020

Keywords:
Thermal energy systems
Microgrids
Seasonal storage
MILP
Investment planning
Piecewise affine function

ABSTRACT

The optimal design of microgrids with thermal energy system requires optimization techniques that can provide investment and scheduling of the technology portfolio involved. In the modeling of such systems with seasonal storage capability, the two main challenges include the low temporal resolution of available data and the non-linear cost versus capacity relationship of solar thermal and heat storage technologies. This work overcomes these challenges by developing two different optimization models based on mixed-integer linear programming with objectives to minimize the total energy costs and carbon dioxide emissions. Piecewise affine functions are used to approximate the non-linear cost versus capacity behavior. The developed methods are applied to the optimal planning of a case study in Austria. The results of the models are compared based on the accuracy and real-time performance together with the impact of piecewise affine cost functions versus non-piecewise affine fixed cost functions. The results show that the investment decisions of both models are in good agreement with each other while the computational time for the 8760-h based model is significantly greater than the model having three representative periods. The models with piecewise affine cost functions show larger capacities of technologies than non-piecewise affine fixed cost function based models.

1. Introduction

The growing attention to decrease the carbon dioxide emissions and at the same time to increase the penetration of renewable energy sources to meet the thermal energy demand require to devise new strategies for the optimal use of technologies such as solar thermal and thermal energy storage. Because of the mismatch between the thermal load (Space Heating and Water Heating) and supply of solar energy in summer, the affordable and carbon footprint-free solar energy has strong potential to meet the thermal energy consumption if the thermal energy storage can be designed optimally to store the heat from solar in summer and use it in winter [1]. The seasonal storage has more advantages in practical applications as compared to short-term storage, but it is challenging since it requires a larger storage volume [1]. The amount of available incident solar radiations on the roof of a typical home exceeds its yearly energy consumption, therefore, there is a large potential in using solar thermal technologies to convert solar radiation into useable heat [2]. The seasonal storage systems have the capability to mitigate the seasonal offset and variation of renewable energy sources.

There are mainly two challenges for the optimal design and operation of a solar thermal system with a large thermal seasonal storage. The first challenge is that the proper modeling techniques require higher resolution of time series data. This challenge of temporal resolution is far more critical when dealing with integration of renewable energy sources [3]. The adequate and appropriate modeling of seasonal storage system requires a time series that spreads over a full year time horizon at least. However, using

* Corresponding author. BEST-Bioenergy and Sustainable Technologies GmbH, Gewerbepark Haag 3, 3250, Wieselburg-Land, Austria.
E-mail addresses: muhammad.mansoor@best-research.eu, mansoor@eeg.tuwien.ac.at (M. Mansoor).

https://doi.org/10.1016/j.energy.2020.119095

Nomenclature

Abbreviations

CPU	central processing unit
DER-CAM	distributed energy resources - customer adoption model
MILP	mixed-integer linear programming
MINLP	mixed-integer nonlinear programming
MPP	monthly peak preservation
OF	objective function
Opt-3D	three daytypes based optimization model
Opt-8760	8760-h based optimization model
PWA	piecewise affine
SOC	state of charge
TRNSYS	transient systems simulation

Mathematical Symbols

δ	binary variable
ε	deviation error (residual)
η	efficiency parameter
λ	non-negative, continuous variable
Π	annuity rate of the technology
Θ	loss factor
ϕ	charging rate of the heat storage
$\overrightarrow{\alpha}$	fit parameter vector
A	technology-specific coefficient, EUR/kW(h)
a	slope of linear segment
$A^{S_{th}}$	decision variable for the solar thermal area, m^2
b	intercept of linear segment
C	costs, EUR
Cap	capacity of the technology to be invested, kW(h)
DER_{invest}	annualized investment cost per distributed energy resource, kW(h)
F	fuel for heat, kWh
FixC	fixed capital cost of the technology, EUR
H	heat variable for different technologies, kWh
I	solar irradiance parameter, W/m^2
n	number of species
T	temperature, °C
VarC	variable capital cost of the technology, EUR/kW(h)
x	technology-specific capacity variable, kW(h)

Superscripts

α	technology-specific exponent
amb	ambient
in	input for storage
loss	loss of stored energy
out	output from storage
stored	state of charge of the storage
S_{th}	solar thermal

Subscripts

char	charge rate of the storage
dis	discharge rate of the storage
HS	heat storage, kWh
O&M	operation and maintenance
st	storage standby operation
s	storage operation
tech	technologies
up	upfront
d	daytypes
h	hours
i	index for binary and decision variables
k	number of components in fit parameter vector
m	months

full year time horizon increases the computational time. In order to solve the issue of computational time, time series aggregation techniques are used to reduce the original full year data into typical design profiles depending upon the aggregation criteria for weekdays, months or seasons. These aggregated design profiles must adequately preserve the significant characteristics of the full year data. Fazlollahi et al. [4] use k-means clustering technique to reduce the yearly time series data into typical periods. Nahmmacher et al. [5] use hierarchical clustering as time series aggregation methodology for solar and wind data. Lozano et al. [6] reduce the time series via averaging into 24-h based profiles defined by weekdays. Averaging into 24-h based profiles defined by months has been studied by Mehleri et al. in Ref. [7]. Averaging into 24-h based profiles defined by seasons has been studied by Samsatli et al. in Ref. [8]. Fahy et al. [9] present the Monthly Peak Preservation (MPP) method to reduce the yearly time series data into three typical periods based on weekdays, weekend days and peak days. Although, the time series aggregation reduces the computational time significantly, it can also change the results as compared to a full year time series optimization [10].

The second challenge lies in the non-linear relationship between the capacity and the cost of technologies involved in thermal energy systems [11]. The real life costs of thermal energy system technologies such as solar thermal and heat storage are dependent on size and larger capacities have lower technology costs. The modeling of this non-linear relationship inside optimization problems imposes certain limits since most of the optimization problems in state-of-the-art literature are formulated as linear programming or mixed-integer linear programming (MILP) problems to keep computational costs and complexity in a reasonable range. Mashayekh et al. [12] use MILP approach to find optimal distributed energy resources in multi-energy system microgrids. Siddiqui et al. [13] use MILP modeling for the heat and power applications. Stadler et al. [14] optimize the distributed energy resources and building retrofits using MILP approach. Steen et al. [15] model the thermal energy storage using MILP framework. Optimal design of energy conversion units and envelopes for residential building retrofits has been studied in Ref. [16] using MILP model. Lindberg et al. [17] propose a methodology for the optimal system design of zero energy buildings using MILP approach. The short-term and long-term thermal energy storage models have been studied using MILP framework in Ref. [18]. In order to solve the issue of non-linear relationship between the capacity and the cost of technologies, piecewise affine (PWA) cost functions can be used instead of non-linear cost functions, but these functions introduce additional decision variables, thus increasing the complexity of models.

Various studies have been carried out in the field of seasonal thermal storage based on simulations in recent years. Böhm and Lindorfer [19] present techno-economic assessment of seasonal heat storage in district heating with different thermo-chemical materials. The socio-economic assessment of seasonal heat storage in district heating systems with waste heat integration has been provided in Ref. [20]. A simulation-based methodology for a

pit seasonal thermal storage with heat pump has been investigated in Ref. [21]. The potential of seasonal solar thermal energy storage using thermo-chemical sorption for domestic application has been studied in Ref. [22]. Ciapmi et al. [23] perform thermo-economic sensitivity analysis by dynamic simulations of solar district heating system with seasonal borehole thermal energy storage. The solar seasonal storage system coupled with ground-source heat pump has been investigated using a simulation for thermal equilibrium in Ref. [24]. Xu et al. [25] demonstrate the potential and evaluate the performance of solar heating system integrated with seasonal energy storage for greenhouse applications. Li et al. [26] present a performance analysis of an integrated energy storage system for seasonal storage and solar thermal energy applications. These simulation-based studies focus on very specific topics related to techno-economic assessment and performance investigation of seasonal storage systems but lack the modeling framework with respect to optimal system design. These studies also provide gaps in realizing the solutions to the challenges faced while modeling the thermal energy systems such as time series aggregation and non-linear cost versus capacity behavior of thermal technologies. Therefore, it is required to focus on addressing these gaps on a system design level so that an optimal planning of thermal energy systems can be realized.

Few studies have been conducted in recent years which are based on optimization in the field of seasonal thermal storage. Launay et al. [27] propose a simplified multi-criteria optimization considering levelized cost of energy as an objective function for a residential building having inter-seasonal solar heat storage. This study does not consider the modeling of costs in terms of piecewise affine functions. Köfinger et al. [28] use a simplified MILP framework considering the minimization of total energy costs for the optimized integration and operation of seasonal heat storage for district heating networks. The optimization problem does not consider the modeling of costs in terms of piecewise affine functions and the modeling details of the seasonal heat storage are also limited in this study. Gabrieli et al. [29] propose two MILP based optimization methods to model a seasonal storage for a multi-energy system by using time series aggregation of a full year data into a set of representative design days given by k-means clustering. This study uses the piecewise affine approximate cost function only for the heat storage technology, but does not consider the piecewiese affine cost function for the solar thermal technology. Kotzur et al. [30] aggregate the time series into a set of representative design periods given by k-means before using them into three different design optimization models. These optimization models do not consider the solar thermal into the technology portfolio and also the non-linear relationship between cost and capacity for the heat storage technology is not modeled as piecewise affine functions. Although k-means is a popular technique to aggregate time series into typical representative periods, preserving the peak demand is critical and requires further implications to maintain the peak of the original demand profile.

The model simplification in using a single linear cost function for solar thermal and heat storage technologies can lead to a significant difference as compared to using a piecewise affine cost function when modeling seasonal thermal energy systems. It is because the seasonal behavior requires larger capacities, and the investment costs for these larger capacities need to be lower when using the correct non-linear cost versus capacity behavior. The modeling of these non-linear cost functions into piecewise affine cost functions has not been addressed in the state of the art studies combinely for solar thermal and seasonal heat storage technologies. Also, the comparison between the investment decisions of the optimization models using the fixed linear (Non-PWA) cost functions and PWA cost functions has not been provided in the state of the art studies. Moreover, longer time horizon based optimization problems have not been discussed extensively at a design phase of storage based thermal energy systems and maintaining the peaks of thermal demand while aggregating the time series is critical to the optimal design of these systems.

Therefore, this research addresses the above mentioned gaps by developing two different MILP optimization models *i.e.* Opt-3D and Opt-8760 for a thermal energy system in a microgrid having central heating, solar thermal and heat storage as technologies. It also includes the essential modeling of non-linear cost functions in terms of piecewise affine (PWA) cost functions for solar thermal and heat storage technologies while keeping the optimization problem as MILP. The Opt-3D model considers the typical profiles based optimization of the system, but preserving the load peaks by the maximum peak preservation method in the daytypes compared to the other works which use k-means clustering. The Opt-8760 model considers the full year time horizon *i.e.* 8760-hours based optimization for the same kind of thermal energy system. The main objective of the MILP framework is to minimize the total energy costs and the total CO_2 emissions. The framework is applied to a case study considering a community residential sector in Austria. The investment and operation of the thermal seasonal storage is presented together with a comparison of results in terms of a relative objective function difference and computational time between two models. Moreover, the investment decision results are also compared based on the PWA and Non-PWA cost functions of both models. This work presents the application of the developed methods to the planning of a case study, quantifying the costs and CO_2 emissions of a reference fuel-based heating system, and showing the cost and CO_2 emission implications of transitioning to a joint solar and fuel-based heating system involving seasonal thermal storage while studying the feasibility *i.e.* solar potential of the necessary heating network for a microgrid.

This paper is structured as follows: Section 2 describes the formulation of the optimization problem for Opt-3D, Opt-8760 and PWA cost functions. Section 3 provides detailed information considering the case study, including pre-processing and analytics of data. Section 4 presents the detailed results. Finally, the conclusions are provided in Section 5.

2. Formulation of optimization problem

This work presents the comparison between two different optimization models using Mixed-Integer Linear Programming (MILP) for thermal energy system, based on DER-CAM [12] and further developed within this research. The MILP minimizes the total annual energy costs or total annual carbon dioxide emissions as separate objective functions and balances the demand by services offered through optimized technology portfolio. The MILP framework, which is used in this study, considers the solar thermal and heat storage as technology options provided that heat from fuels *i.e.* central heating grid is always available to meet the marginal heating demand when solar thermal and heat storage technologies are not available. Since the optimization is based on MILP, piecewise affine functions are used to model the costs associated with the solar thermal and heat storage technologies to approximate the non-linear behavior.

2.1. Opt-3D: optimization model with uncoupled representative days

The first model uses time series aggregation to reduce the yearly data into 24-h based three representative daytypes for each month by using monthly peak preservation method [9]. The daytypes

include week, peak and weekend representative profiles. The choice of these three different daytypes in each month is considered because the thermal load has variation in the consumption pattern within week days and weekend days of each month. Therefore average profile of this different consumption within four weeks of each month requires two representative daytypes to capture the variation of week days and weekend days. As averaging the consumption within week days and weekend days lowers the original maximum demand, therefore peak days are required in each month which can preserve the maximum of demand in each hour of the month so that the optimization decisions are made by keeping into account the original maximum demand within each month. The peak profiles are generated by taking the maximum of demand in every hour of all days in the month. The week day and weekend day profiles are then generated by subtracting the peak demand value in the hour of week days and weekend days where that maximum occurred. The subtraction of the peak demand values depends upon the occurrence of that maximum in original week day or weekend day. Finally, all the demand values of week days and weekend days are summed up over hours and then divided by the number of the respective original week days and weekend days less one (considering one peak day per month) in that particular month. It is because of the separation of the peak demand values from these week days and weekend days that average values must be adjusted downwards to maintain the monthly total consumption in reasonable range. The time horizon is disintegrated into hours $h \in \{1, 2, \ldots, 24\}$, daytypes $d \in \{1, 2, 3\}$ and months $m \in \{1, 2, \ldots, 12\}$. The optimization takes every decision variable into account for each time-step h within each daytype d of every month m. The monthly and annual quantities are scaled up by using the number of the days $n_{m,d}$ (such that $\sum_{m=1}^{12}\sum_{d=1}^{3} n_{m,d} = 365$) for each daytype in every month.

The simplified objective function related to the total annual energy costs C can be represented by eq. (1).

$$C = \sum_{\text{tech}} DER_{\text{invest}} + \sum_{m,d,h} C_{\text{utility}} + \sum_{m,d,h} C_{\text{O\&M}} \tag{1}$$

where DER_{invest} is the annualized investment cost per technology *tech*, C_{utility} is related to volumetric fuel costs and other fixed costs related to utility and $C_{\text{O\&M}}$ is related to the operation and maintenance costs. DER_{invest} can be further described as shown in eq. (2).

$$DER_{\text{invest}} = \sum_{\text{tech}} (C_{\text{up}}\ \Pi_{\text{tech}}) \tag{2}$$

$$C_{\text{up}} = VarC_{\text{tech}}\ Cap_{\text{tech}} + FixC_{\text{tech}} \tag{3}$$

where C_{up} is the upfront capital cost of the technology, Π_{tech} is the annuity rate of the technology, $VarC_{\text{tech}}$ is the variable capital cost of the technology, Cap_{tech} is the technology capacity to be invested, $FixC_{\text{tech}}$ are the fixed capital costs of the technology. The variable capital costs vary with the amount of capacity that is invested, while the fixed capital costs are independent on the size of the technology and cover engineering costs.

The simplified objective function related to the total annual carbon dioxide emissions can be represented by eq. (4). It is the summation of the carbon dioxide emissions from burning different fuel types used in providing the heat.

$$CO_2 = \sum_{\text{fueltype}} \sum_{m,d,h} CO_2\text{fuels} \tag{4}$$

The heat received from the solar thermal is given by eq. (5).

$$H^{S_{\text{th}}}_{m,d,h} = A^{S_{\text{th}}}\ I_{m,h}\ \eta^{S_{\text{th}}}_{m,h} \tag{5}$$

where $A^{S_{\text{th}}}$ is the decision variable for the solar thermal area, $I_{m,h}$ is the parameter for the solar irradiance modeled based on [31] and $\eta^{S_{\text{th}}}_{m,h}$ is the parameter for the solar thermal efficiency modeled according to Ref. [32]. For Opt-3D model, the solar irradiance and solar thermal efficiency are modeled by weather data that are averaged on monthly basis over hours and the resulting heat from the solar decision variable assumes the same output for all the three daytypes in each month.

The heat storage model is defined by eqs. (6)–(9).

$$H^{\text{stored}}_{m,d,h} = H^{\text{stored}}_{m,d,h-1} + H^{\text{in}}_{m,d,h} - H^{\text{out}}_{m,d,h} - H^{\text{loss}}_{m,d,h} \tag{6}$$

$$H^{\text{in}}_{m,d,h} = H^{\text{for}}_{m,d,h}\ \eta_{\text{char}} \tag{7}$$

$$H^{\text{out}}_{m,d,h} = H^{\text{from}}_{m,d,h}\ 1 \Big/ (\eta_{\text{dis}}) \tag{8}$$

$$H^{\text{loss}}_{m,d,h} = H^{\text{stored}}_{m,d,h-1}\ \Theta_{\text{s}} + Cap_{\text{HS}}\ \Theta_{\text{st}}\ \frac{\left(T_{\min} - T^{\text{amb}}_{m,h}\right)}{(T_{\max} - T_{\min})} \tag{9}$$

where $H^{\text{stored}}_{m,d,h}$ represents the state of the charge of the heat storage, $H^{\text{in}}_{m,d,h}$ is the input for heat storage, $H^{\text{for}}_{m,d,h}$ is the heat required for storing in heat storage, η_{char} is the charging efficiency, $H^{\text{out}}_{m,d,h}$ is the output from heat storage, $H^{\text{from}}_{m,d,h}$ is the heat required from the heat storage, η_{dis} is the discharging efficiency, $H^{\text{loss}}_{m,d,h}$ is the heat lost in heat storage during working and standby conditions, Θ_{s} is the loss factor during storage operation, Θ_{st} is the loss factor during storage standby condition, Cap_{HS} is the capacity of the heat storage, $T_{\min}$ is the minimum temperature of the storage, $T_{\max}$ is the maximum temperature of the storage and $T^{\text{amb}}_{m,h}$ is the ambient temperature. The heat storage model constraints are given by eq. 10–13.

$$H^{\text{stored}}_{m,d,1} = H^{\text{stored}}_{m,d,24} + H^{\text{in}}_{m,d,1} - H^{\text{out}}_{m,d,1} - H^{\text{loss}}_{m,d,1} \tag{10}$$

$$H^{\text{stored}}_{m,d,h} \le Cap_{\text{HS}} \tag{11}$$

$$H^{\text{in}}_{m,d,h} \le Cap_{\text{HS}}\ \phi^{\max}_{\text{char}} \tag{12}$$

$$H^{\text{out}}_{m,d,h} \le Cap_{\text{HS}}\ \phi^{\max}_{\text{dis}} \tag{13}$$

where eq. (10). represents the periodicity constraint in dynamic condition and shows that the first hour of the state of the charge of heat storage is linked with the last hour of the respective daytype d in the month m of the state of the charge of heat storage. $\phi^{\max}_{\text{char}}$ is the maximum charging rate of the heat storage and $\phi^{\max}_{\text{dis}}$ is the maximum discharging rate of the heat storage. The higher level energy balance can be represented in a simplified manner by eq. (14).

$$H^{\text{load}}_{m,d,h} + H^{\text{for}}_{m,d,h} = H^{S_{\text{th}}}_{m,d,h} + H^{\text{from}}_{m,d,h} + H^{\text{fuels}}_{m,d,h} \tag{14}$$

where $H^{\text{load}}_{m,d,h}$ is the thermal load of the system to be satisfied and $H^{\text{fuels}}_{m,d,h}$ is associated with the fuel for heat $F^{\text{heat}}_{m,d,h}$ by an efficiency parameter represented by η_{fuel} as given in eq. (15).

$$H^{\text{fuels}}_{m,d,h} = \eta_{\text{fuel}}\, F^{\text{heat}}_{m,d,h} \tag{15}$$

2.2. Opt-8760: optimization model with 8760-hours time horizon

Since the Opt-3D model considers the time series aggregation and the resulting representative daytype profiles, it does not keep any connectivity between the optimization days, and thus, can not model the seasonal storage behavior directly. The Opt-8760 model uses a full scale yearly time horizon *i.e.* 8760-hours and increases the time resolution of the MILP model used in Opt-3D by replacing $m \in \{1, 2, \ldots, 12\}$, $d \in \{1, 2, 3\}$ and $h \in \{1, 2, \ldots, 24\}$ with $t \in \{1, 2, \ldots, 8760\}$ for all the demand as well as the weather input data. This full scale optimization considers connectivity between all the optimization time-steps and can therefore model seasonal storage behavior directly.

2.3. Piecewise affine cost functions for solar thermal and heat storage

The cost functions of the technologies that are used in thermal systems *i.e.* solar thermal and heat storage are not always justified as linear functions [11]. The costs of large hot water heat storage systems are dominated by the material for the tank since the storage capacity is proportional to the volume of the tank. A simple dimensional analysis demonstrates that for the most common type of heat storages (hot water tanks), an approximate power-law given by eq. (16) can be used when comparing typical costs for storage tanks [11]. Similarly, the costs of large solar thermal systems are observing non-linearities with its capacity and can be represented as given in eq. (16) [33]:

$$C_{\text{up}}(x) = A\, x^{\alpha} \tag{16}$$

where $C_{\text{up}}(x)$ is the non-linear cost function, x is the capacity of the solar thermal or heat storage and A and α are the technology-specific parameters (e.g. $A = 0.661$ [Million-EUR/MW] and $\alpha = 0.835$ for solar thermal [33] and $A = 141$ [EUR/kWh] and $\alpha = 0.667$ for heat storage [11]).

A Piecewise Affine (PWA) linear approximation approach is used in this study to model the non-linear cost function $C_{\text{up}}(x)$ for both solar thermal and heat storage technologies as compared to other works which only consider heat storage technology for PWA approximations. This is in particular desirable because mixed integer non-linear programming (MINLP) problems can be translated into the MILP problems for which efficient algorithms and optimization software packages are widely available. In general, PWA functions consist of several discrete linear segments (pieces) that are used to describe a univariate function $f(x)$. The location where one of these linear segments ends and a new one begins are designated as breakpoints x_i. A PWA linear function $\tilde{f}(x)$ can be described as the following set of linear equations:

$$\tilde{f}(x) = \begin{cases} a_1(x - x_1) + b_1 & x_1 < x \le x_2 \\ a_2(x - x_2) + b_2 & x_2 < x \le x_3 \\ \vdots & \vdots \\ a_{n-1}(x - x_{n-1}) + b_{n-1} & x_{n-1} < x \le x_n \end{cases} \tag{17}$$

where a_i are the slopes, b_i are the intercepts of the different linear segments, n is the number of breakpoints x_i and $(n - 1)$ represents the total number of linear segments. A schematic illustration of a PWA approximation function $\tilde{f}(x)$ with three linear pieces of an arbitrary non-linear function $f(x)$ is demonstrated in Fig. 1. A fundamental issue in modeling non-linear functions for MILP problems is how to represent the PWA approximation function $\tilde{f}(x)$ as a set of linear equations using discrete and continuous decision variables [34]. This issue is addressed in this study by using the Convex Combination Model [35] to represent PWA approximation functions $\tilde{f}(x)$.

2.3.1. Convex combination model

The convex combination model represents the PWA approximation functions $\tilde{C}_{\text{up}}(x)$ as a linear combination of the breakpoints x_i as given in eq. 18 and 19.

$$\tilde{C}_{\text{up}}(x) = \sum_{i=1}^{n} \lambda_i\, C_{\text{up}}(x_i) \tag{18}$$

$$x = \sum_{i=1}^{n} \lambda_i\, x_i \tag{19}$$

where all coefficients λ_i are non-negative, continuous variables between 0 and 1 and summed up to 1 as given in eq. 20 and 21.

$$\lambda_i \in [0, 1],\ i = 1, \ldots, n \tag{20}$$

$$\sum_{i=1}^{n} \lambda_i = 1 \tag{21}$$

The constraints related to λ_i are given in eq. (22).

$$\lambda_i \le \begin{cases} \delta_{i+1} & \text{for } i = 0 \\ \delta_i + \delta_{i+1} & \text{for } i = 1, \ldots, n-1 \\ \delta_i & \text{for } i = n \end{cases} \tag{22}$$

where δ_i are binary variables and are modeled as given in eq. 23 and 24.

$$\delta_i \in \{0, 1\},\ i = 1, \ldots, n \tag{23}$$

$$\sum_{i=1}^{n} \delta_i = 1 \tag{24}$$

The binary variables δ_i and the listed constraints given by eq. (22) enforce the condition that at the most two weighting factors λ_i are non-zero, in which case they must be adjacent. Therefore, if the binary variable $\delta_{i+1} = 1$ for instance, then the point $(x, \tilde{C}_{\text{up}}(x)) = (\lambda_i\, x_i,\ \lambda_i\, C_{\text{up}}(x_i)) + (\lambda_{i+1}\, x_{i+1},\ \lambda_{i+1}\, C_{\text{up}}(x_{i+1}))$ is given by the linear (convex) combination of the two points $(x_i,\ C_{\text{up}}(x_i))$ and $(x_{i+1},\ C_{\text{up}}(x_{i+1}))$ since $\lambda_i + \lambda_{i+1} = 1$ and $0 \le \lambda_i \le (\delta_i + \delta_{i+1}) = 1$,

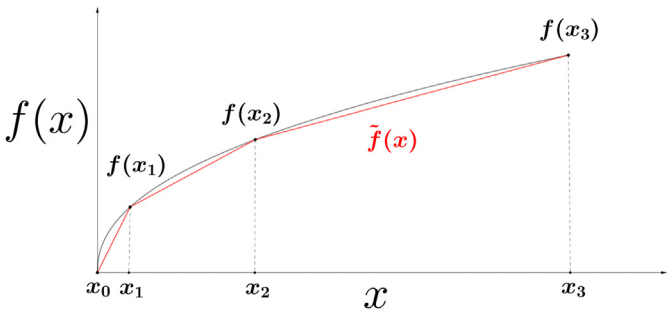

Fig. 1. A schematic illustration of the PWA approximation function $\tilde{f}(x)$ with three linear pieces.

$\lambda_{i+1} \geq 0.$

2.3.2. Fitting non-linear cost functions

The optimal positions of the breakpoints x_i are not always known. Moreover, a simple linear connection using just the convex combination model between the original cost function values $C_{\text{up}}(x_i)$ leads to a PWA approximation $\tilde{C}_{\text{up}}(x)$, where the functional values are systematically smaller than that of $C_{\text{up}}(x)$ *i.e.* $\tilde{C}_{\text{up}}(x) \leq C_{\text{up}}(x) : \forall x$ except at the breakpoint locations x_i where $C_{\text{up}}(x_i) = \tilde{C}_{\text{up}}(x_i)$. Therefore, performing a linear fit process before using the convex combination model minimizes the deviation errors (residuals) $\varepsilon_i = |C_{\text{up}}(x_i) - \tilde{C}_{\text{up}}(x_i)|$. In this study, a preliminary analysis is performed using logarithmically spaced separation which suggests that at least five linear segments are needed to cover five orders of magnitude for heat storage and solar thermal with a deviation error of less than 10%. Thus, the linear fit process is performed by considering $n = 6$ breakpoints (five linear segments) and minimizing the sum-of-squares of the residuals ε_i as given in eq. (25).

$$\min_{\vec{\alpha}} \sum_{i=1}^{n} \left(C_{\text{up}}(x_i) - \tilde{C}_{\text{up}}(x_i; \vec{\alpha}) \right)^2 = \min_{\vec{\alpha}} \sum_{i=1}^{n} \varepsilon_i^2 \tag{25}$$

where the components $(\alpha_1, \ldots, \alpha_k)$ of the vector $\vec{\alpha} \in \mathbb{R}^k$ are the fit parameters of the linear segments. The regression analysis method is performed several times for five continuous linear pieces until the minimum deviation error is found.

After performing the linear fit process, the PWA approximation functions $\tilde{C}_{\text{up}}(x)$ are modeled through the convex combination model as described in Section 2.3.1. The resulting PWA parameters for solar thermal and heat storage technologies are given in Table 1. Depending upon the capacity chosen by the optimization model, the respective linear segment of the piecewise affine function is activated and the costs are calculated using the variable cost and fixed costs of that active linear segment. The cost vs. capacity curves using linear cost functions, non-linear cost functions and PWA cost functions for solar thermal and heat storage technologies are illustrated in Fig. 2 and Fig. 3 respectively. It can be seen from Figs. 2 and 3 that the upfront capital costs of solar thermal as well as heat storage technologies are significantly lower for the large capacities considering the resulting linearly fitted piecewise affine function as compared to just single linear cost function.

Table 1
Investment parameters for solar thermal and heat storage technologies with piecewise affine (PWA) cost functions. The non-linear cost functions are considered according to Ref. [11,33].

Parameter	Solar Thermal	Heat Storage
Min. Cap.	0 [kW]	0 [kWh]
Breakpoint 12	350 [kW]	350 [kWh]
Breakpoint 23	4238 [kW]	3500 [kWh]
Breakpoint 34	11,443 [kW]	35,000 [kWh]
Breakpoint 45	21,741 [kW]	350,000 [kWh]
Max. Cap.	35,000 [kW]	3,500,000 [kWh]
Cost Value at Min. Cap.	0 [€]	520 [€]
Cost Value at Breakpoint 12	345,884.14 [€]	6820 [€]
Cost Value at Breakpoint 23	2,249,511.90 [€]	33,119.88 [€]
Cost Value at Breakpoint 34	5,092,805.40 [€]	155,206.46 [€]
Cost Value at Breakpoint 45	8,675,353.80 [€]	722,005.19 [€]
Cost Value at Max. Cap.	12,893,566 [€]	3,350,130.58 [€]
Fixed Costs of Linear Segment 1	0 [€]	520 [€]
Fixed Costs of Linear Segment 2	174,511.57 [€]	3897.79 [€]
Fixed Costs of Linear Segment 3	577,170.54 [€]	19,554.70 [€]
Fixed Costs of Linear Segment 4	1,112,048.18 [€]	92,228.82 [€]
Fixed Costs of Linear Segment 5	1,758,462.20 [€]	429,991.26 [€]
Variable Cost of Linear Segment 1	988.24 [€/kW]	18 [€/kWh]
Variable Cost of Linear Segment 2	489.64 [€/kW]	8.35 [€/kWh]
Variable Cost of Linear Segment 3	397.62 [€/kW]	3.88 [€/kWh]
Variable Cost of Linear Segment 4	347.88 [€/kW]	1.80 [€/kWh]
Variable Cost of Linear Segment 5	318.15 [€/kW]	0.83 [€/kWh]

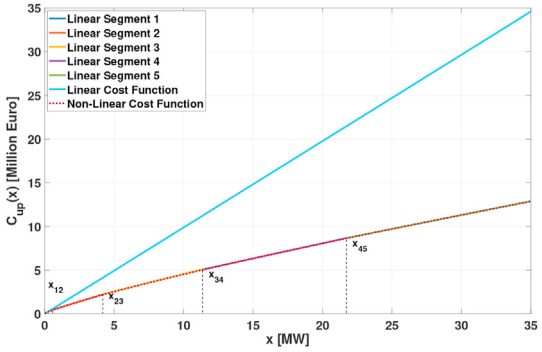

Fig. 2. Cost vs. Capacity curve of solar thermal technology using linear, non-linear and PWA cost functions.

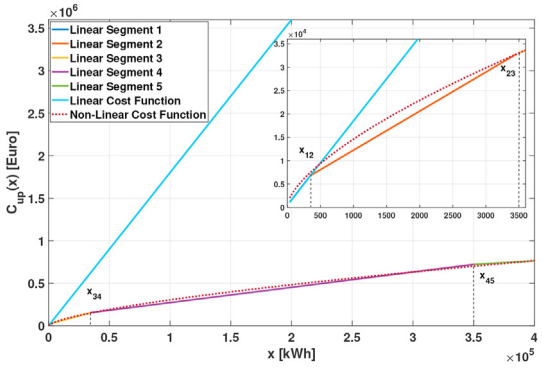

Fig. 3. Cost vs. Capacity curve of heat storage technology using linear, non-linear and PWA cost functions.

3. Case study

This section covers the general overview of the approach to the definition of the case study, data analytics and pre-processing. The case study is related to a set of community residential buildings in Austria. Only space heating load is considered for this study and it is generated using TRNSYS [36] simulations on hourly basis for a whole year. Central heating through biomass fuel, solar thermal and heat storage technologies are considered to satisfy the thermal load. The heat storage considered for this study is a hot water tank storage. The schematic diagram of the researched thermal system is illustrated in Fig. 4.

3.1. Time series data analysis and processing

The hourly load profile of the thermal load for the whole year is demonstrated in Fig. 5. The thermal load profile shown in Fig. 5 is also used directly in the Opt-8760 model. The annual load is around 2004 MWh/a with a peak load of 2 MW_p. The seasonal behavior is clearly evident from Fig. 5 and shows no load in the summer months.

The yearly profile is then reduced by time series aggregation as mentioned in Section 2.1. This results in 24-h based three representative daytypes *i.e.* week, peak and weekend for all the 12 months. The resulting representative profiles are shown in Fig. 6

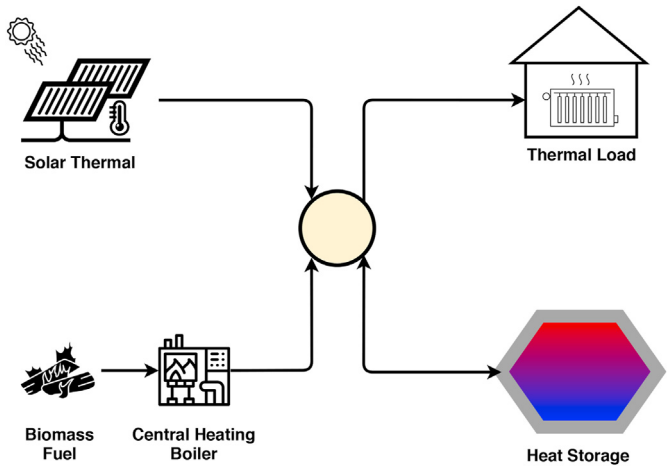

Fig. 4. Schematic diagram of investigated thermal system.

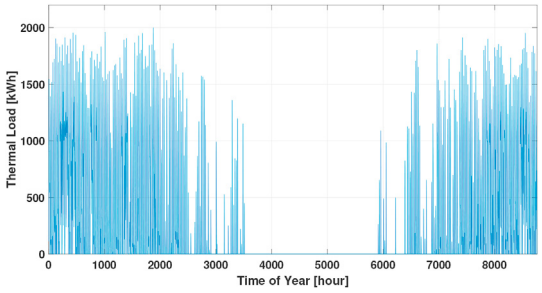

Fig. 5. Thermal load profile on hourly basis for all the year [36].

and are used for the Opt-3D model. It can be seen from Fig. 6 (b) that the peaks for every month are preserved and the week and weekend profiles are averaged after subtracting the peaks form the respective occurring daytypes. The number of the days for the week, peak and weekend daytypes are selected according to Table 2. The total annual thermal load based on these number of days associated with respective profiles results in 2003 MWh/a, a 0.05% difference relative to the original yearly thermal demand, with the same peak load of 2 MW_p. This shows that the time series aggregation method captures the monthly variations adequately in terms of week days, weekend days and peak days so that the percentage difference between the original yearly thermal demand and the up-scaled yearly thermal demand from the reduced representative profiles in each month is almost negligible.

The weather data include the global irradiance, diffuse irradiance and ambient temperature. These data are gathered through Meteonorm [37] for the location of the considered case study. The weather data are available for one full year on hourly time-steps and used for the Opt-8760 model. The hourly based weather data are shown in Fig. 7. These weather data are also reduced using time series aggregation method to get average values per month for Opt-3D model and are shown in Fig. 8.

3.2. Techno-economical parameters

The economic parameters for both Opt-3D and Opt-8760 optimization models are the same. These include the investment parameters such as fixed capital costs, variable capital costs, fixed maintenance costs, lifetime and annuity rate. The fixed and variable capital costs for solar thermal and thermal storage are different when considering the fixed linear *i.e.* Non-PWA cost functions and

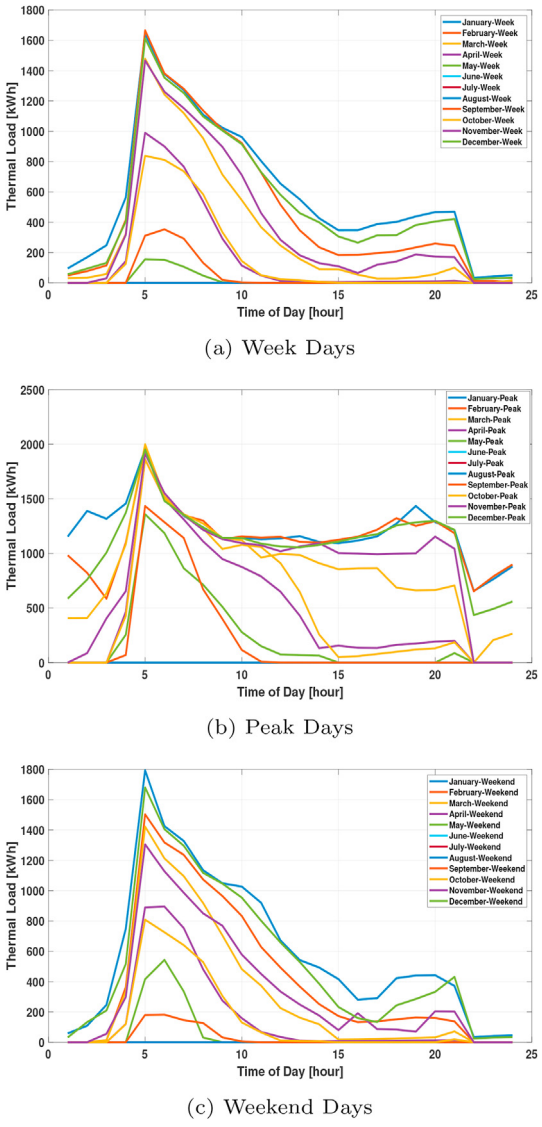

Fig. 6. Time series aggregated representative profiles of the thermal load for all the year.

Table 2
Number of the days for representative profiles in each month.

Month	Week Days	Peak Days	Weekend Days
January	21	1	9
February	19	1	8
March	22	1	8
April	20	1	9
May	22	1	8
June	21	1	8
July	21	1	9
August	22	1	8
September	20	1	9
October	21	1	9
November	21	1	8
December	21	1	9

PWA cost functions. The economic parameters for central heating, solar thermal and heat storage considering Non-PWA fixed cost functions are reported in Table 3 based on [38,39]. The economic parameters for solar thermal and heat storage considering the PWA cost functions are given in Table 1 as mentioned in Section 2.3.2.

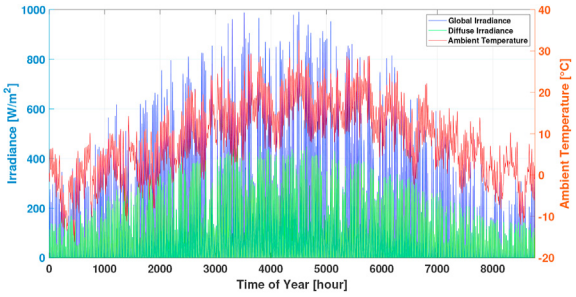

Fig. 7. Weather Data: Global Irradiance, Diffuse Irradiance and Ambient Temperature on hourly basis for all the year [37].

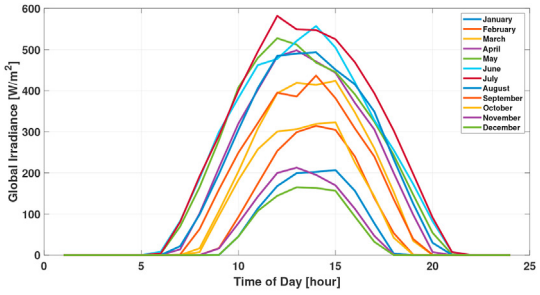

(a) Global Irradiance

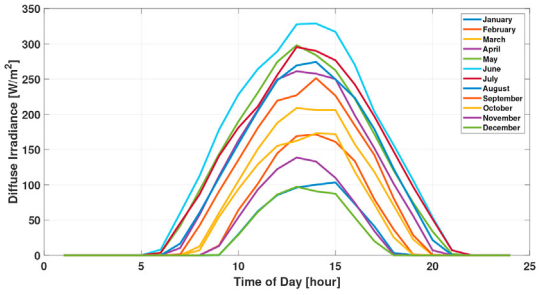

(b) Diffuse Irradiance

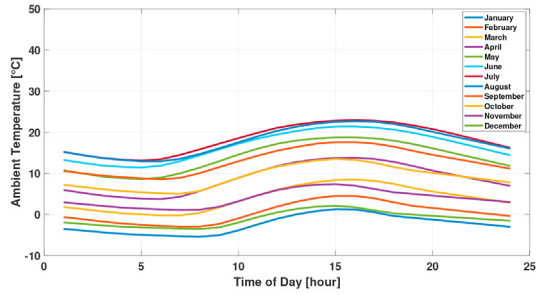

(c) Ambient Temperature

Fig. 8. Time series aggregated representative profiles of weather parameters for all the year.

Table 4
Technical parameters for heat storage [15,18,40].

Parameter	Value
η_{char} [%]	90
η_{dis} [%]	90
ϕ_{char}^{max} [%]	75
ϕ_{dis}^{max} [%]	75
T_{min} [°C]	15
T_{max} [°C]	65
Θ_s/Θ_{st} [%]	Opt-3D: 0.08 Opt-8760: 0.01

The solar thermal collectors have horizontal orientation with a tilt angle of 20°. The technical parameters for the heat storage contain the charging and discharging efficiencies, maximum charge and discharge rates, minimum and maximum temperatures and losses. These parameters are same for the Opt-3D and the Opt-8760 models except the parameters of losses. The losses for the Opt-8760 model are assumed in accordance with [18]. Whereas, the losses for the Opt-3D model are assumed to be 8% higher than the Opt-8760 model given that the Opt-3D is a non-seasonal model and the losses for short-term non-seasonal heat storage are higher than the long-term seasonal storage [40]. These parameters are given in Table 4 and are based on [15,18,40].

The technical parameters for the central heating contain the fueltype, volumetric fuel costs, fuel to heat efficiency and marginal CO_2 emissions. These parameters are based on [38] and are given in Table 5. The biomass based central heating technology does not consider the minimum output constraint in terms of production mode and the optimizer chooses the optimal capacity based on the maximum $H_{m,d,h}^{fuels}$ output as defined by the eq. (15).

3.3. Optimization & testing framework

For testing the case study, the Opt-3D and the Opt-8760 optimization models are tested for different scenarios reported in Table 6.

Scenario-0 is the basecase where the central heating technology is only considered for supplying to the load and no heat storage and solar thermal technologies are allowed. The optimal total energy costs and total CO_2 emissions are calculated for both models by using cost minimization. These costs and CO_2 emissions are then taken as reference for the rest of scenarios and objective function savings. Costs and CO_2 emissions are calculated relative to these references in the respective cost and CO_2 optimization runs for

Table 5
Technical parameters for central heating [38].

Parameter	Value
Fueltype	Biomass
Fuel Costs [€/kWh]	0.05
η_{fuel} [%]	78
CO_2 Fuel Emissions [kg CO_2 /kWh]	0.02

Table 3
Investment parameters for central heating, solar thermal and heat storage technologies with fixed linear (Non-PWA) cost function [38,39].

Technology	Fixed Cost	Variable Costs	Fixed Maintenance Costs	Lifetime	Annuity Rate
	[€]	[€/kW] or [€/kWh]	[€/kW] or [€/kWh] per month	[Years]	[%]
Central Heating	13,821	270	1.72	25	5.74
Solar Thermal	0	988	0	20	6.72
Heat Storage	520	18	0	25	5.74

Table 6
Different scenarios for the optimization and testing framework.

Scenario	Optimization Model	Minimization
Scenario-0 (a): Basecase	Opt-3D	Cost
Scenario-0 (b): Basecase	Opt-8760	Cost
Scenario-1 (a): 0% relaxation w.r.t basecase	Opt-3D	Cost
Scenario-1 (b): 0% relaxation w.r.t basecase	Opt-3D	CO_2
Scenario-2 (a): 0% relaxation w.r.t basecase	Opt-8760	Cost
Scenario-2 (b): 0% relaxation w.r.t basecase	Opt-8760	CO_2
Scenario-3: 50% relaxation w.r.t basecase	Opt-3D	CO_2
Scenario-4: 50% relaxation w.r.t basecase	Opt-8760	CO_2

Scenario-1 to Scenario-4. Scenario-1 includes the cost and CO_2 minimization using the Opt-3D model with 0% relaxation to their respective reference costs and CO_2 emissions. A 0% relaxation means that the objective function from the optimization case cannot be higher than the one from the reference case. Scenario-2 includes the cost and CO_2 minimization using the Opt-8760 model with 0% relaxation to their respective reference costs and CO_2 emissions. Scenario-3 and Scenario-4 include the CO_2 minimization using the Opt-3D and the Opt-8760 models respectively with 50% relaxation in the reference costs, meaning that the objective functions can be 50% higher than the one in the reference cases, allowing for more progressive results. Scenario-1 to Scenario-4 are tested by considering fixed linear (Non-PWA) cost functions as well as PWA cost functions for both models. The results are compared based on the investment decisions by the optimizer, objective function savings, absolute run time, objective function difference and the run time savings between both the Opt-3D and the Opt-8760 models for all scenarios. The optimality gap of the optimization solver was set to 0.2% for all the scenarios. The MILP optimization for both models was performed on a server with a 6 core Intel Xeon E5-1650 v3 CPU @ 3.5 GHz and 192 GB of RAM.

4. Results

This section provides the comparison between the results of all scenarios given in Table 6. The resulting investment decisions chosen by the optimizer for all the scenarios are reported in Table 7. The objective function difference and the run time savings between both the Opt-3D and the Opt-8760 models relative to the Opt-8760 model are reported in Table 8 and illustrated in Fig. 9.

The results of scenario-0 (a) and scenario-0 (b) indicate that the total energy costs and the total CO_2 emissions are almost same for both the Opt-3D and the Opt-8760 models with an objective function difference of 0.02%. These two scenarios set the reference case for the next scenarios. This also indicates that the time series aggregation method used is effective when reducing the data into three representative daytypes.

When considering 0% relaxation in the reference case, the cost minimization in scenario-1 (a) and scenario-2 (a) invests in a small amount of solar thermal and heat storage technologies, but this reduces the capacity of central heating and provides almost the same objective function savings for both models and just 1.78% objective function difference using Non-PWA cost functions. With

Table 7
Results of the investment decisions of all scenarios for both the Opt-3D and the Opt-8760 models using fixed linear (Non-PWA) cost functions as well as piecewise affine (PWA) cost functions.

	Scenarios	Model	Min.	OF Costs [k€]	OF CO2 [tons]	Central Heating [kWh]	Solar Thermal [kW]	Heat Storage [kWh]	OF Savings [%]	Run Time [s]
	Scenario-0 (a)	Opt-3D	Cost	194.02	59.05	2000	–	–	–	0.81
	Scenario-0 (b)	Opt-8760	Cost	194.06	59.07	2000	–	–	–	8.03
Non-PWA	Scenario-1 (a)	Opt-3D	Cost	183.44	59.05	1612	8	2791	5.45	2.06
	Scenario-1 (b)	Opt-3D	CO_2	194.02	58.92	1643	31	10,717	0.22	2.59
	Scenario-2 (a)	Opt-8760	Cost	180.01	59.07	1411	20	5701	7.24	81.3
	Scenario-2 (b)	Opt-8760	CO_2	194.06	58.5	1406	63	17,839	0.98	91.64
	Scenario-3	Opt-3D	CO_2	291.02	58.2	1675	262	90,045	1.44	2.11
	Scenario-4	Opt-8760	CO_2	291.08	54.73	1380	358	101,101	76.6	49.52
PWA	Scenario-1 (a)	Opt-3D	Cost	179.36	59.05	1389	44	15,186	7.56	3.14
	Scenario-1 (b)	Opt-3D	CO_2	194.02	58.55	1479	143	49,138	0.85	3.38
	Scenario-2 (a)	Opt-8760	Cost	173.37	59.07	1148	70	19,655	10.66	177.47
	Scenario-2 (b)	Opt-8760	CO_2	194.06	54.45	814	569	160,471	7.83	361.59
	Scenario-3	Opt-3D	CO_2	291.02	57.97	2046	497	170,875	1.83	2.11
	Scenario-4	Opt-8760	CO_2	291.08	13.82	191	4512	1,500,870	76.6	224.91

Table 8
Results of objective function difference and run time savings between Opt-3D and Opt-8760 models relative to Opt-8760 model for different scenarios. Scenario-0 (a), Scenario-1 (a), Scenario-1 (b) and Scenario-3 consider the Opt-3D model. Scenario-0 (b), Scenario-2 (a), Scenario-2 (b) and Scenario-4 consider the Opt-8760 model.

	Scenarios	Min.	OF Difference [%]	Run Time Savings [%]
	Scenario-0 (a) & Scenario-0 (b)	Cost	0.02	89.91
Non-PWA	Scenario-1 (a) & Scenario-2 (a)	Cost	1.78	97.47
	Scenario-1 (b) & Scenario-2 (b)	CO_2	0.76	97.17
	Scenario-3 & Scenario-4	CO_2	5.91	95.74
PWA	Scenario-1 (a) & Scenario-2 (a)	Cost	3.1	98.23
	Scenario-1 (b) & Scenario-2 (b)	CO_2	6.98	99.07
	Scenario-3 & Scenario-4	CO_2	74.77	99.06

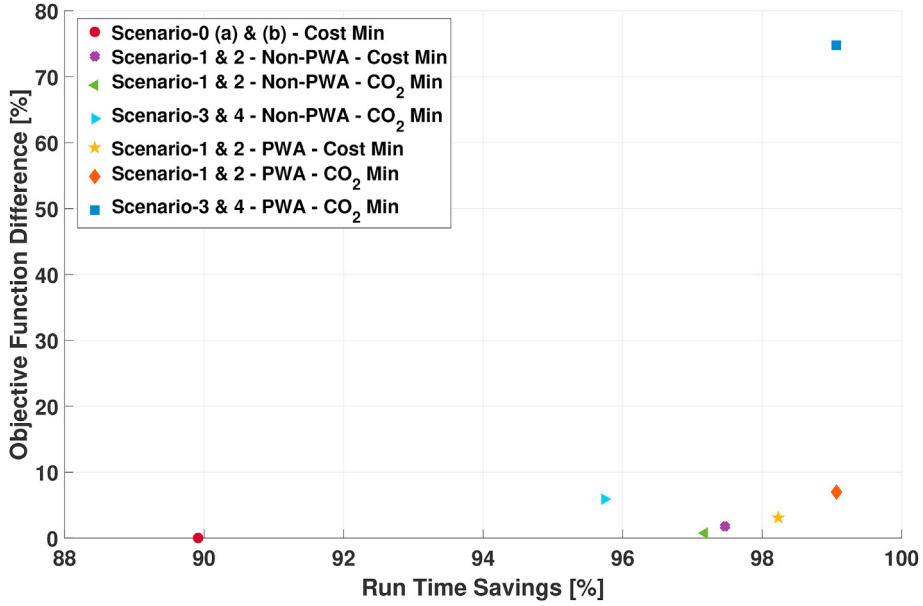

Fig. 9. Comparison between the results of objective function difference and run time savings between Opt-3D and Opt-8760 models relative to Opt-8760 model for different scenarios.

PWA cost functions, the objective function savings in scenario-1 (a) and scenario-2 (a) are higher than that of Non-PWA cost functions for both models but the objective function difference is also higher than that of Non-PWA.

When considering 0% relaxation in the reference case, the CO_2 minimization in scenario-1 (b) invests more in solar thermal and heat storage as compared to its cost minimization runs, but even this amount of solar thermal and heat storage is not effective since objective function savings are almost insignificant (less than 1%) using either Non-PWA or PWA cost functions. The size of heat storage is not big enough to be qualified for the seasonal storage as the volume of 849 m^3 related to the biggest capacity of 49,138 kWh in scenario-1 (b) using PWA cost functions is less than the practical range of seasonal heat storage volume [41]. This is also true for the CO_2 minimization in scenario-2 (b) using Non-PWA cost functions which invests in heat storage capacity of 17,839 kWh (equivalent to 308 m^3 of volume). Whereas, the CO_2 minimization in scenario-2 (b), which uses Opt-8760 model, invests in bigger capacities of solar thermal and heat storage and lower capacity of central heating using PWA cost functions as compared to its Non-PWA run which can be considered as seasonal storage with 7.83% of CO_2 savings. The objective function difference between scenario-1 (b) and 2 (b) using PWA for CO_2 minimization run is 6.98% which is higher than that of the Non-PWA optimization run.

When considering 50% relaxation in the reference costs and Non-PWA cost functions, the CO_2 minimization in scenario-3 using Opt-3D model and scenario-4 using Opt-8760 model have an objective function difference of 5.91%. The sizes of the solar thermal and heat storage are bigger than in the previous respective scenarios as the costs are relaxed thus moving towards the expensive bigger systems for seasonal storage. Even though the size of the heat storage is comparable between both two models, which is a surprising result due to the lack of connectivity between the daytypes in the Opt-3D model, the daytype model is not able to transfer the energy provided by solar thermal in summer months and shift it to winter months, thus increasing the objective function difference relative to the Opt-8760 model. This result indicates that when considering the Opt-3D model, it can provide the investment decisions in a good agreement with the Opt-8760 model with reduced run time, when specific constraints and assumptions are made.

When considering 50% relaxation in the reference costs and PWA cost functions, the CO_2 minimization in scenario-3 using Opt-3D model does invest in bigger capacities for solar thermal and heat storage, but due to the lack of connectivity between the daytypes, these bigger capacities are not able to provide significant objective function savings as compared to that of scenario-4 using Opt-8760 model. The results of scenario-4 with PWA cost functions indicate a huge reduction in central heating capacity followed by the big investments in solar thermal and heat storage capacities. This is because of the use of the PWA functions, which considers lower costs for higher capacities of these technologies. The objective function savings are about 76.6% with a 1.5 GWh capacity of heat storage (25,918 m^3) and a 4512 kW capacity of solar thermal (5679 m^2 of solar collector field area). The resulting optimal dispatch of scenario-4 using the PWA cost functions is demonstrated in Fig. 10. The dispatch results of scenario-4 using the PWA cost functions show the seasonal effect of the heat storage by storing the energy in summer months and using the stored heat in winter months.

5. Conclusion

This work considers the development of two different optimization models *i.e.* Opt-3D and Opt-8760 with a different time horizon using MILP modeling framework. The first model uses the time series aggregation methods to reduce the yearly data into three different representative daytypes. The second model considers the full scale time horizon for the same data. The MILP framework considers the minimization of the total annual energy costs and the total annual CO_2 emissions of a thermal energy system having central heating, solar thermal and heat storage as technologies for a case study comprising of eight different scenarios. The non-linear costs related to the technology investments for solar thermal and heat storage technologies are linearized into piecewise affine (PWA) cost functions by using linear fit process and convex combination model. Both of the optimization models consider the fixed linear (Non-PWA) cost functions as well as PWA

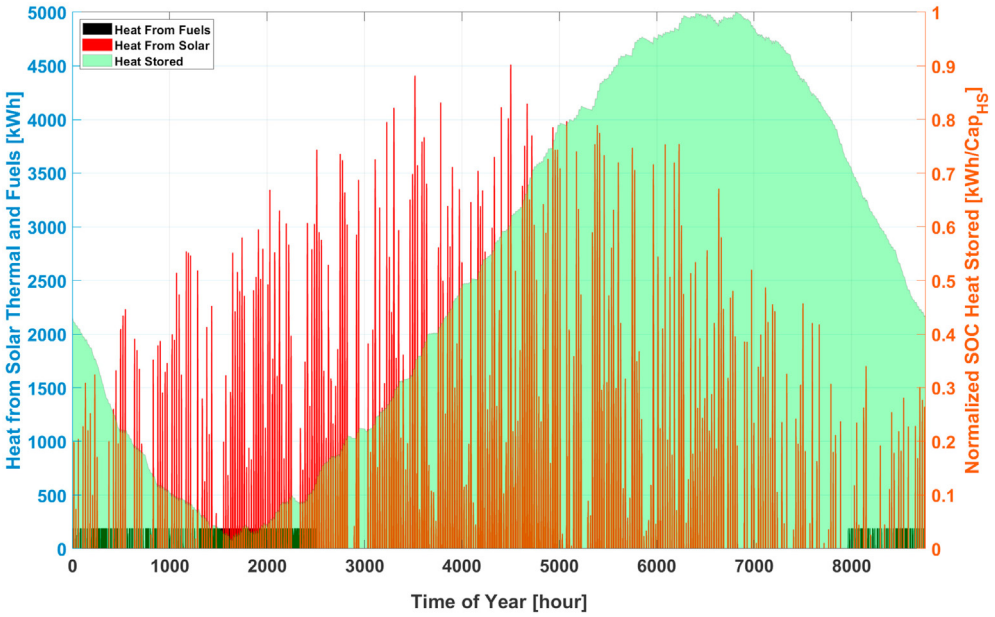

Fig. 10. Optimal dispatch for Scenario-4: 50% relaxation w.r.t basecase considering the Opt-8760 model with CO_2 minimization using piecewise affine (PWA) cost functions.

cost functions for solar thermal and heat storage technologies in all scenarios. A detailed testing and validation of the Opt-3D and the Opt-8760 models have been presented by assessing the accuracy of the time series aggregation methodology and comparing the investment decisions, the objective function savings, the objective function difference and the run time of both models in all scenarios using fixed linear (Non-PWA) cost functions as well as PWA cost functions.

In summary, the Opt-3D and the Opt-8760 models provide comparable results in cost minimization by both using Non-PWA and PWA cost functions for Scenario-1 and Scenario-2 respectively. The investment decision results for CO_2 minimization using Non-PWA cost functions for the Opt-3D model in scenario-1 and scenario-3 are well aligned with the investment decision results for CO_2 minimization using Non-PWA cost functions for the Opt-8760 model in scenario-2 and scenario-4 respectively. However, these investment decisions vary significantly when considering the CO_2 minimization using PWA cost functions in scenario-1 to scenario-4 with Opt-8760 model performing better than the Opt-3D model by providing bigger investments in solar thermal and heat storage technologies, thus contributing to a maximum of 76.6% CO_2 savings. In all the scenarios, the Opt-3D model has significant run time savings as compared to the Opt-8760 model because of its lower time resolution. This can be considered a positive result for the cost minimization in scenario-1 and scenario-2 and also in the CO_2 minimization in scenario-1 to scenario-4 using Non-PWA cost functions, since the results do not deviate significantly in terms of objective function difference. But, for scenario-3 and scenario-4, better results are observable at the cost of bigger run time by using the Opt-8760 model. Furthermore, the run time is higher for the optimization runs in all scenarios using PWA cost functions as compared to that of using Non-PWA cost functions due to additional decision variables in both optimization models.

These results show that the seasonal behavior of heat storage in a thermal energy system can have a significant effect when considering the full scale optimization modeling using piecewise affine cost functions, but the computational run time for solving the optimization model can be significantly larger. Therefore, further work is necessary to develop an understanding on how the optimal seasonal storage planning can be achieved by using models like the Opt-3D, but with connected daytypes, and present a comparison between the optimal sizing and dispatch of technology portfolio, objective function accuracy and computational resources. Also, the water heating demand can be considered together with space heating demand depending upon the application of the system under study and can increase the computational effort for both models because of the additional model variables and equations.

Credit author statement

Muhammad Mansoor: Conceptualization, Methodology, Software, Writing - Review & Editing. **Michael Stadler:** Conceptualization, Methodology, Supervision, Resources, Writing - Review & Editing. **Michael Zellinger:** Visualization, Project administration. **Klaus Lichtenegger:** Methodology, Formal analysis. **Hans Auer:** Investigation, Resources. **Armin Cosic:** Methodology, Software, Data Curation, Writing - Review & Editing.

Declaration of competing interest

The authors declare that they have no known competing financial interests or personal relationships that could have appeared to influence the work reported in this paper.

Acknowledgements

The authors would like to acknowledge SOLID, an Austrian solar engineering company specializing in all aspects of large-scale solar thermal energy plants, for the valuable discussions on this topic. This research work was funded by the Austrian Research and Promotion Agency (FFG) under the project *OptEnGrid* (grant no. 858815) and also by the the province of Lower Austria under the project *Grundlagenforschung Smart und Microgrids* (grant no. K3-F-755/001–2017).

References

[1] Xu J, Wang RZ, Li Y. A review of available technologies for seasonal thermal

energy storage. Sol Energy 2014;103:610–38.
[2] Pinel P, Cruickshank CA, Beausoleil-Morrison I, Wills A. A review of available methods for seasonal storage of solar thermal energy in residential applications. Renew Sustain Energy Rev 2011;15(7):3341–59.
[3] Pfenninger S. Dealing with multiple decades of hourly wind and PV time series in energy models: a comparison of methods to reduce time resolution and the planning implications of inter-annual variability. Appl Energy 2017;197:1–13.
[4] Fazlollahi S, Bungener SL, Mandel P, Becker G, Maréchal F. Multi-objectives, multi-period optimization of district energy systems: I. Selection of typical operating periods. Comput Chem Eng 2014;65:54–66.
[5] Nahmmacher P, Schmid E, Hirth L, Knopf B. Carpe diem: a novel approach to select representative days for long-term power system modeling. Energy 2016;112:430–42.
[6] Lozano MA, Ramos JC, Carvalho M, Serra LM. Structure optimization of energy supply systems in tertiary sector buildings. Energy Build 2009;41(10):1063–75.
[7] Mehleri ED, Sarimveis H, Markatos NC, Papageorgiou LG. Optimal design and operation of distributed energy systems: application to Greek residential sector. Renew Energy 2013;51:331–42.
[8] Samsatli S, Staffell I, Samsatli NJ. Optimal design and operation of integrated wind-hydrogen-electricity networks for decarbonising the domestic transport sector in Great Britain. Int J Hydrogen Energy 2016;41(1):447–75.
[9] Fahy K, Stadler M, Pecenak ZK, Kleissl J. Input data reduction for microgrid sizing and energy cost modeling: representative days and demand charges. J Renew Sustain Energy 2019;11(6):065301.
[10] Kotzur L, Markewitz P, Robinius M, Stolten D. Impact of different time series aggregation methods on optimal energy system design. Renew Energy 2018;117:474–87.
[11] Lichtenegger K, Unterberger V. Thermal trouble: challenges in optimization and evaluation of thermal energy systems. Oxford, United Kingdom: IAPE'19; 2019.
[12] Mashayekh S, Stadler M, Cardoso G, Heleno M. A mixed integer linear programming approach for optimal DER portfolio, sizing, and placement in multi-energy microgrids. Appl Energy 2017;187:154–68.
[13] Siddiqui AS, Firestone RM, Ghosh S, Stadler M, Edwards JL, Marnay C. Distributed energy resources customer adoption modeling with combined heat and power applications. 2003.
[14] Stadler M, Groissböck M, Cardoso G, Marnay C. Optimizing distributed energy resources and building retrofits with the strategic DER-CAModel. Appl Energy 2014;132:557–67.
[15] Steen D, Stadler M, Cardoso G, Groissböck M, DeForest N, Marnay C. Modeling of thermal storage systems in MILP distributed energy resource models. Appl Energy 2015;137:782–92.
[16] Schütz T, Schiffer L, Harb H, Fuchs M, Müller D. Optimal design of energy conversion units and envelopes for residential building retrofits using a comprehensive MILP model. Appl Energy 2017;185:1–15.
[17] Lindberg KB, Doorman G, Fischer D, Korpås M, Ånestad A, Sartori I. Methodology for optimal energy system design of Zero Energy Buildings using mixed-integer linear programming. Energy Build 2016;127:194–205.
[18] Renaldi R, Friedrich D. Multiple time grids in operational optimisation of energy systems with short-and long-term thermal energy storage. Energy 2017;133:784–95.
[19] Böhm H, Lindorfer J. Techno-economic assessment of seasonal heat storage in district heating with thermochemical materials. Energy 2019;179:1246–64.
[20] Moser S, Mayrhofer J, Schmidt RR, Tichler R. Socioeconomic cost-benefit-analysis of seasonal heat storages in district heating systems with industrial waste heat integration. Energy 2018;160:868–74.
[21] Sorknæs P. Simulation method for a pit seasonal thermal energy storage system with a heat pump in a district heating system. Energy 2018;152:533–8.
[22] Ma Z, Bao H, Roskilly AP. Seasonal solar thermal energy storage using thermochemical sorption in domestic dwellings in the UK. Energy 2019;166:213–22.
[23] Ciampi G, Rosato A, Sibilio S. Thermo-economic sensitivity analysis by dynamic simulations of a small Italian solar district heating system with a seasonal borehole thermal energy storage. Energy 2018;143:757–71.
[24] Liu L, Zhu N, Zhao J. Thermal equilibrium research of solar seasonal storage system coupling with ground-source heat pump. Energy 2016;99:83–90.
[25] Xu J, Li Y, Wang RZ, Liu W. Performance investigation of a solar heating system with underground seasonal energy storage for greenhouse application. Energy 2014;67:63–73.
[26] Li T, Wang R, Kiplagat JK, Kang Y. Performance analysis of an integrated energy storage and energy upgrade thermochemical solidgas sorption system for seasonal storage of solar thermal energy. Energy 2013;50:454–67.
[27] Launay S, Kadoch B, Le Métayer O, Parrado C. Analysis strategy for multi-criteria optimization: application to inter-seasonal solar heat storage for residential building needs. Energy 2019;171:419–34.
[28] Köfinger M, Schmidt RR, Basciotti D, Terreros O, Baldvinsson I, Mayrhofer J, Moser S, Tichler R, Pauli H. Simulation based evaluation of large scale waste heat utilization in urban district heating networks: optimized integration and operation of a seasonal storage. Energy 2018;159:1161–74.
[29] Gabrielli P, Gazzani M, Martelli E, Mazzotti M. Optimal design of multi-energy systems with seasonal storage. Appl Energy 2018;219:408–24.
[30] Kotzur L, Markewitz P, Robinius M, Stolten D. Time series aggregation for energy system design: modeling seasonal storage. Appl Energy 2018;213:123–35.
[31] Duffie John A, Beckman William A. Solar engineering of thermal processes/John A. Duffie. William A. Beckman Wiley New York; 1991.
[32] European solar Thermal Industry Federation (ESTIF). Simple calculation of energy delivery of (small) ST systems (Report). 2007. retrieved at: http://www.estif.org/fileadmin/estif/content/policies/downloads/SimpleCalculation.pdf.
[33] Grosse R, Christopher B, Stefan W, Geyer R, Robbi S. Long term (2050) projections of techno-economic performance of large-scale heating and cooling in the EU. Luxemburg: Publications Office of the European Union; 2017.
[34] Camponogara E, de Almeida KC, Junior RH. Piecewise-linear approximations for a non-linear transmission expansion planning problem. IET Gener, Transm Distrib 2015;9(12):1235–44.
[35] Nemhauser GL, Wolsey LA. Integer and combinatorial optimization. New York: john wiley & sons; 1988. p. 118.
[36] Klein SA, et al. TRNSYS 18: a transient system simulation program. Madison, USA: Solar Energy Laboratory, University of Wisconsin; 2017. http://sel.me.wisc.edu/trnsys.
[37] Remund J, Müller S, Kunz S, Schilter C. METEONORM: global meteorological database for solar energy and applied climatology. Meteotest; 2007.
[38] Hartmann H, Reisinger K, Thuneke K, Höldrich A, Roßmann P. Handbuch bioenergie-kleinanlagen. 2013.
[39] Samweber F, Schifflechner C. Kostenanalyse wärmespeicher bis 10.000 l speichergröße - stand dezember 2016. Forschungsstelle für Energiewirtschaft e.V; 2017.
[40] Mangold LDD, Deschaintre L. Task 45 Large Systems-Seasonal thermal energy storage Report on state of the art and necessary further R+ D. In: International energy agency solar heating and cooling programme; 2015.
[41] Mangold D, Schmidt T, Dohna A, Späh D. Guideline for seasonal thermal energy storage systems in the built environment. Solites; 2016.